

## Influence of interfacial hydrogen and oxygen on the Schottky barrier height of nickel on (111) and (100) diamond surfaces

J. van der Weide and R. J. Nemanich

*Department of Physics, North Carolina State University, Raleigh, North Carolina 27695-8202*

(Received 9 June 1993; revised manuscript received 21 October 1993)

In this paper we report on Schottky barrier height measurements of nickel on both diamond (111) and (100) surfaces, as a function of surface preparation. The Schottky barriers of thin ( $< 5 \text{ \AA}$ ) nickel films on natural type-IIb (*p*-type semiconducting) diamond (111) and (100) surfaces were determined with ultraviolet photoemission spectroscopy. Exposing the diamond (111) surfaces to an argon plasma while heated to  $350^\circ\text{C}$  resulted in a change from a negative-electron-affinity surface to a positive-electron-affinity surface. This effect was used as an indication that a hydrogen-free surface had been obtained. Deposition of a monolayer of nickel on the hydrogen-free diamond (111) surface resulted in a Schottky barrier height of 0.5 eV. The nickel caused the surface to exhibit a negative-electron-affinity surface. Nickel deposited on a diamond (111) surface with a negative electron affinity, indicative of a monohydride-terminated surface, resulted in a  $\sim 1.0$ -eV Schottky barrier height. Diamond (100) surfaces were prepared by vacuum annealing to temperatures ranging from  $500^\circ\text{C}$  to  $1070^\circ\text{C}$ . The various anneals resulted in a lowering of the electron affinity by up to  $\sim 1$  eV, which resulted in a negative electron affinity after the surface had been annealed to  $\sim 1000^\circ\text{C}$ . Oxygen was initially present on the surface but could not be observed after the  $1000^\circ\text{C}$  anneal. The removal of oxygen and the appearance of a negative electron affinity coincided with the appearance of a  $2 \times 1$  surface reconstruction. Nickel was deposited after the various anneals, and Schottky barrier heights were found, ranging from 1.5 eV for the  $545^\circ\text{C}$ -annealed surface to 0.7 eV for the  $1070^\circ\text{C}$ -annealed surface. These measurements suggest that for both the (111) and the (100) diamond surfaces the presence of chemisorbed species, such as hydrogen and oxygen, results in an increase in the Schottky barrier height.

### I. INTRODUCTION

Diamond exhibits unique electronic properties, such as a wide band gap (5.47 eV, high carrier mobilities ( $\mu_n = 2200 \text{ cm}^2/\text{V s}$ ,  $\mu_p = 1600 \text{ cm}^2/\text{V s}$ ) and a high breakdown field ( $10^7 \text{ V/cm}$ ), which combine to make diamond an excellent semiconductor material to be used for high-speed, high-temperature, or high-power transistors. Various field-effect transistors (FET's)<sup>1-5</sup> and bipolar junction transistors<sup>6,7</sup> based on diamond have been reported. Most of these experimental devices are made from expensive natural diamond. The development of chemical-vapor-deposition growth of diamond increases its potential to become an economically viable electronic material. In order to make use of diamond in device technology both Ohmic and rectifying contacts will be needed. At present only *p*-type diamond can be reliably produced, and Schottky barriers may play an important role as an alternative for the *p-n* junction. Because of this the metal-diamond interface has been studied more intensely in recent years.<sup>8-29</sup> The general trend that emerges in these studies is that the as-deposited metal contacts exhibit rectifying behavior. However, significant variation in the measured Schottky barrier heights is observed. Several studies have indicated that the rectifying properties are dependent on surface preparation.<sup>15,23</sup>

In this paper we report on Schottky barrier height measurements of nickel on both diamond (111) and (100) surfaces, as a function of surface preparation. Nickel has

a fcc crystal structure which closely matches the lattice constant of diamond ( $a_{\text{dia}} = 3.567 \text{ \AA}$ ,  $a_{\text{Ni}} = 3.523 \text{ \AA}$ ), and it is possible to grow nickel epitaxially on diamond (111) and (100) surfaces.<sup>18,30,31</sup> Theoretical investigations of the diamond-nickel interface have been performed by Erwin and Pickett<sup>32-35</sup> and Pickett, Pederson, and Erwin.<sup>36</sup> Their calculations are focused on two different structures for nickel on both the (111) and the (100) surfaces. These structures are shown in Fig. 1. For both the (111) and the (100) surface a Schottky barrier of less than 0.1 eV is found for the most stable configurations. It should, however, be noted that these are calculations of nickel on idealized diamond surfaces, and the presence of chemisorbed species is not taken into account. Calculations on the effects of hydrogen on the Schottky barrier height have been performed by Lambrecht for the copper-diamond (111) interface.<sup>37</sup> For copper on the hydrogen-free diamond surface Lambrecht reports a Schottky barrier height of less than 0.1 eV, which is similar to the results found by Erwin and Pickett for nickel on the diamond (111) surface. Lambrecht found, however, that the presence of hydrogen at the copper-diamond interface resulted in an increased Schottky barrier height of  $\geq 1.0$  eV.

The diamond (111) surface is typically terminated by a monohydride after the surface has been polished and etched.<sup>38-41</sup> The presence of the monohydride on the surface is found to lower the work function of the surface, which causes the diamond (111) surface to exhibit a negative electron affinity.<sup>39,41</sup> This means that electrons that are at the conduction-band minimum have sufficient

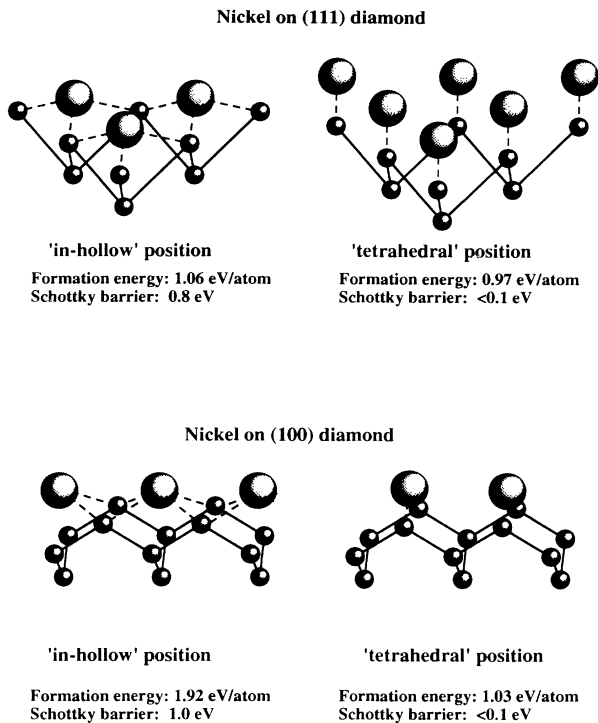
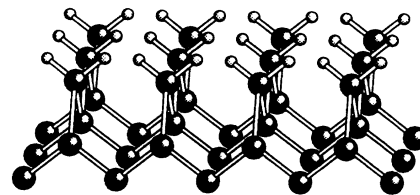


FIG. 1. Various configurations of nickel on diamond (111) and (100) as studied in Refs. 32–34, and 36.

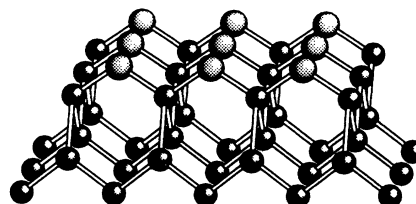
energy to overcome the work function. The presence of a negative electron affinity can be detected with photoemission spectroscopy, since secondary electrons that are thermalized to the conduction-band minimum are emitted and appear as a sharp peak in the spectra.<sup>39–47</sup> The hydrogen can be removed from the diamond (111) surface by annealing the surface to  $>950^\circ\text{C}$ , which typically results in a  $2 \times 1/2 \times 2$  reconstructed surface with a positive electron affinity. We have recently shown that a positive-electron-affinity surface can also be achieved by heating the surface to  $350^\circ\text{C}$  while exposing it to an argon plasma for several minutes.<sup>48</sup>

The ideal diamond (100) surface has two dangling bonds, and it has been suggested that the unreconstructed diamond (100) surface is terminated by a dihydride, as illustrated in Fig. 2(a).<sup>49</sup> Theoretical calculations have indicated that it might be difficult to achieve this surface structure due to steric repulsion between the hydrogen atoms.<sup>50–52</sup> Hydrogen and oxygen desorption and adsorption studies performed by Thomas, Rudder, and Markunas suggest that a partial oxygen termination can also result in a  $1 \times 1$  surface structure.<sup>53</sup> A schematic of possible bonding configurations is shown in Figs. 2(b) and 2(c). The diamond (100) surface is observed to reconstruct to a  $2 \times 1$  structure after the surface is annealed to  $\sim 1000^\circ\text{C}$ . Theoretical calculations indicate that a monohydride-terminated surface is energetically more favorable than a hydrogen-free surface, and is therefore the most likely structure for the (100)  $2 \times 1$  reconstructed surface in the presence of atomic hydrogen.<sup>50–52</sup>

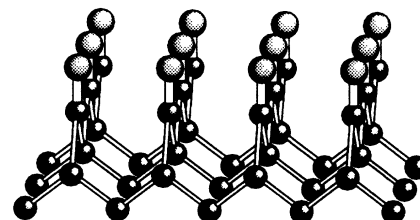
Schottky barrier height measurements have been made for various metals on diamond. Using current-voltage,



(a) Diamond (100)  $1 \times 1$ :2H Dihydride structure



(b) Diamond (100)  $1 \times 1$ :O Bridging structure



(c) Diamond (100)  $1 \times 1$ :O Double-bonded structure

FIG. 2. (a) Dihydride- and (b) and (c) oxygen-terminated diamond (100) surfaces with a  $1 \times 1$  surface structure.

capacitance-voltage, and photoresponse methods, Mead and McGill have found Schottky barrier heights ranging from 1.8 to 2.0 eV for gold, 1.9 to 2.2 eV for aluminum, and 2.0 eV for barium.<sup>54</sup> The diamond surfaces were obtained by cleaving, followed by an etch in various chemical solutions such as chromic acid and HF, and a rinse in distilled water. Based on photoemission-spectroscopy measurements, Himpfel and co-workers report Schottky barrier heights of 1.3 eV for gold and 1.5 eV for aluminum on unreconstructed diamond (111).<sup>43,45</sup> The diamond surfaces in their study were prepared by the method proposed by Lurie and Wilson,<sup>30</sup> which consists of polishing the surface with diamond grit, followed by an ultrasonic acetone rinse and a  $\sim 900^\circ\text{C}$  anneal in vacuum. This resulted in a negative electron affinity, indicative of a hydrogen-terminated diamond (111) surface. Significant differences exist in the Schottky barrier heights reported by the two groups. However, both groups find that the Schottky barrier heights of the various metals on the diamond (111) surface are virtually independent of the work function and electron affinity of the metals used. The lowest Schottky barrier height on the (111) surface, 1.0 eV, was found by van der Weide and Nemanich for titanium on an argon-plasma-cleaned surface.<sup>55,56</sup> This surface exhibited a positive electron affinity prior to metal deposition and was presumed to be free of hydrogen.<sup>48</sup>

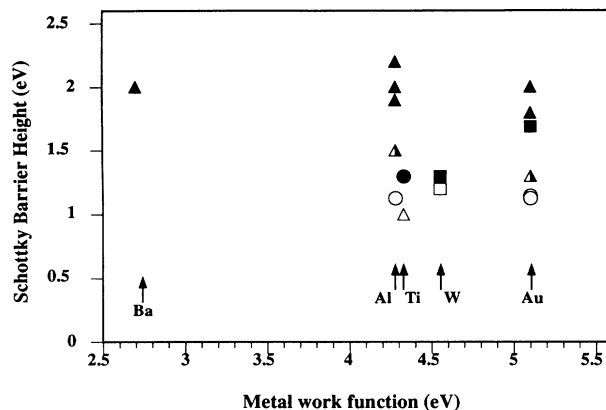


FIG. 3. Summary of Schottky barrier heights reported in the literature. The triangles represent Schottky barrier heights obtained from (111) surfaces, the squares represent data from (100) surfaces, and the circles are Schottky barrier heights on polycrystalline diamond film. A black symbol indicates an *ex situ* chemical surface preparation while the open symbols represent *in vacuo* prepared surfaces. The half-filled triangles represent data for metal on a hydrogen-terminated (111) surface.

Schottky barrier heights for metals on the diamond (100) surface include a value of 1.7 eV, reported by Glover for gold on synthetic diamond, which was cleaned in a boiling mixture of  $\text{H}_2\text{SO}_4$  and  $\text{KNO}_3$ .<sup>14</sup> Geis *et al.* obtained a barrier height of 1.3 eV for tungsten contacts on diamond (100) from current-voltage measurements.<sup>10</sup> Their surface preparation consisted of an etch in a saturated solution of  $\text{CrO}_3$  in  $\text{H}_2\text{SO}_4$  followed by an etch in  $\text{H}_2\text{O}_2$  and  $\text{NH}_4\text{OH}$ . A similar value of 1.2 eV was found by Shiomi *et al.* for tungsten on epitaxially grown, (100)-oriented diamond films.<sup>25</sup>

Tachibana, Williams, and Glass report a value of 1.3 eV for titanium on polycrystalline diamond film which is observed to reduce to 0.8 eV after annealing to 430 °C for 30 min.<sup>27</sup> The diamond film was cleaned in a mixture of  $\text{HNO}_3$ ,  $\text{H}_2\text{SO}_4$ , and  $\text{HClO}_4$ . A Schottky barrier height of 1.13 eV for gold and aluminum on as-grown polycrystalline diamonds films was found by Hicks *et al.*,<sup>16</sup> almost identical to the 1.15-eV Schottky barrier height found by Grot *et al.* for gold on a similar surface.<sup>29</sup>

The various Schottky barrier heights are summarized in Fig. 3 as a function of the work function of the metal. No clear dependence can be discerned between the work function of the metal and the Schottky barrier height. There is, however, a relation between surface preparation and Schottky barrier height, which suggests that surfaces cleaned in vacuum (open symbols) result in a lower Schottky barrier height than surfaces which have been chemically cleaned (solid symbols).

## II. EXPERIMENTAL

The experiments described here were performed in the vacuum system depicted in Fig. 4. The system consists of four chambers, a plasma-cleaning chamber, a chamber for low-energy electron diffraction (LEED) and Auger

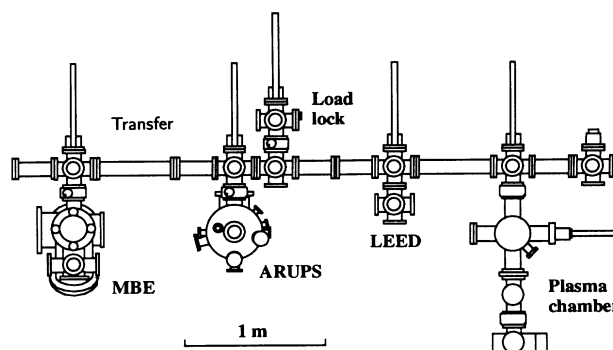


FIG. 4. Schematic of the vacuum equipment used in the experiments.

electron spectroscopy (AES), an angle-resolved ultra-violet photoemission spectroscopy (ARUPS) chamber, and a molecular-beam epitaxy (MBE) chamber. Samples can be moved to the various chambers by means of a vacuum transfer system consisting of a rail-mounted sample holder. A load lock allows the introduction of samples without corrupting the vacuum.

Schottky barrier height measurements were performed in the ARUPS chamber. Photoemission is excited by He I radiation (21.21 eV) generated in a differentially pumped noble-gas-discharge lamp. Photoemitted electrons, emitted at surface normal, are measured with a 50-mm-radius hemispherical electron analyzer with a 0.15-eV energy resolution and a 2° angular resolution. The sample stage is electrically isolated from the rest of the chamber and was biased by up to 1 V in order to allow low-energy electrons to overcome the work function of the analyzer. The Schottky barrier height ( $\phi_b$ ) can be determined from photoemission spectra by locating the valence-band edge ( $E_v$ ) of the semiconductor and the Fermi level ( $E_F$ ) of the metal in the spectra as is shown in Fig. 5. For the (111) surface the position of the valence-

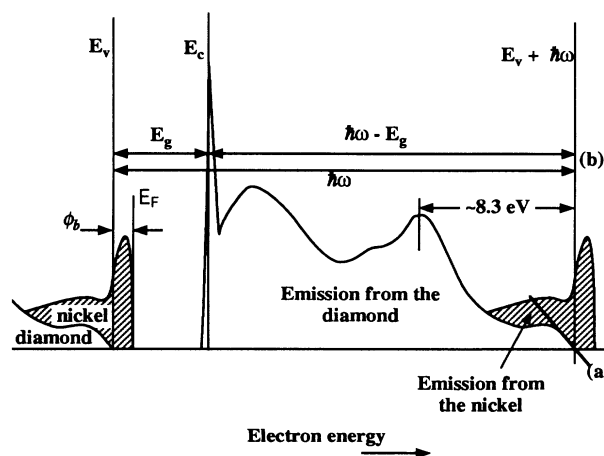


FIG. 5. The Schottky barrier height is determined from the relative positions of the metal Fermi level ( $E_F$ ), and valence-band edge ( $E_v$ ). The latter can be determined by linear extrapolation of the onset of emission [method (a)] or deduced from the negative-electron-affinity peak ( $E_c$ ) which indicates the position of the conduction-band edge [method (b)].

band edge can be determined by linearly extrapolating the onset of the emission to zero as shown in the figure at (a). An independent means of establishing the position of the valence-band edge is available when the surface exhibits a negative electron affinity. In that case the vacuum level lies below the conduction-band edge ( $E_c$ ) and secondary electrons that have thermalized to the bottom of the conduction-band edge are emitted. This results in a sharp peak indicating the position of the conduction-band edge ( $E_v$ ). The position of the valence-band edge in the spectrum can be deduced by adding  $\hbar\omega - E_g$  to the position of the peak, as shown in Fig. 5 at (b).

The experiments are limited to thin metal films ( $< 5 \text{ \AA}$ ), since the determination of the Schottky barrier height from photoemission measurements relies on the presence of features due to both the metal and the underlying semiconductor. Even at low metal coverages it is not always possible to determine the position of the valence-band edge accurately from the spectra, since emission from the metal obscures the relatively weak semiconductor valence-band emission. The valence-band edge was therefore determined from the spectrum of the diamond before metal deposition and related to a stronger emission feature which remained visible after metal deposition. In our experiments a feature at 8.3 eV below the valence-band edge was used. The position of this feature was found by fitting a Gaussian curve to a selected range of data points. A similar feature was found in spectra obtained from the (100) surface. A negative-electron-affinity peak on the (100) surface was used to confirm that the feature also occurred at 8.3 eV below the valence-band edge in the (100) spectra. At low metal coverages the onset of emission at the Fermi level is not as abrupt as for complete metal films. Linear extrapolation of the onset of emission was therefore used to determine the position of the Fermi level of the metal overlayer.

The diamond substrates used in this study were commercially supplied natural diamond obtained from Dubbeldee Harris. It was found necessary to use the *p*-type semiconducting variety of diamond (type IIb), since non-conducting diamond samples (type IIa) did not yield a signal. This is attributed to charging. The diamond substrates measured  $3 \times 3 \times 0.5 \text{ mm}^3$  or  $4 \times 4 \times 0.5 \text{ mm}^3$ , with typical resistivities of  $\sim 10^4 \text{ } \Omega \text{ cm}$ . The surfaces of two of these substrates were oriented to within  $4^\circ$  of the (111) planes, while the two other substrates were (100) oriented to within  $2^\circ$ . The substrates were polished with  $0.1\text{-}\mu\text{m}$  diamond grit and chemically cleaned before every experiment. The chemical clean consisted of a 10-min etch in boiling sulfuric acid to remove wax and residues from the polishing process. This was followed by 30 min in a boiling, saturated solution of  $\text{CrO}_3$  in sulfuric acid to remove graphitic carbon from the surface. The clean was concluded with a 10-min etch in boiling *aqua regia* to remove metallic traces and a deionized-water rinse. Just before the substrates were loaded into the vacuum they were given a final hand polish with dry lens paper. Once in vacuum the diamond (111) substrates were annealed to temperatures up to  $850^\circ\text{C}$  for 10 min in order to desorb contaminants. After the anneals the substrates were

heated to  $350^\circ\text{C}$  and exposed for 10 min to an argon plasma in the plasma chamber to remove hydrogen bonded to the surface.<sup>48</sup> After each plasma exposure, the sample was transferred to the ARUPS chamber, where the absence of the peak associated with a negative-electron-affinity surface was used to indicate that the plasma had removed the hydrogen from the surface. The diamond (100) substrates were given the same *ex situ* treatment as the diamond (111) substrates. Once in vacuum the diamond (100) substrates were exposed to 10-min anneals, ranging in temperature from  $545^\circ\text{C}$  to  $1070^\circ\text{C}$ .

Nickel was deposited in the MBE chamber, in  $\sim 0.5\text{-}\text{\AA}$  increments. After each deposition a photoemission spectrum was obtained in the ARUPS chamber. Typical evaporation rates were  $\sim 10 \text{ \AA/min}$  with the sample at ambient temperatures. The sample was not heated in order to reduce island formation and to obtain complete coverage. Epitaxial growth is not expected to occur under those conditions.<sup>31</sup> Both scanning electron microscopy (SEM) and scanning tunneling microscopy (STM) measurements were attempted to determine the film morphology. However, the resolution of the SEM was limited due to sample charging and the STM images were too noisy for the same reason. Neither of these measurements yielded interpretable results.

### III. RESULTS

#### A. Nickel on diamond (111)

The photoemission spectra as a function of nickel thickness were obtained from an argon-plasma-cleaned diamond (111) surface and are shown in Fig. 6. The spectra obtained after nickel deposition show the emerging Fermi edge of the nickel as the thickness of the nickel film is increased. In addition, a peak at the low-energy

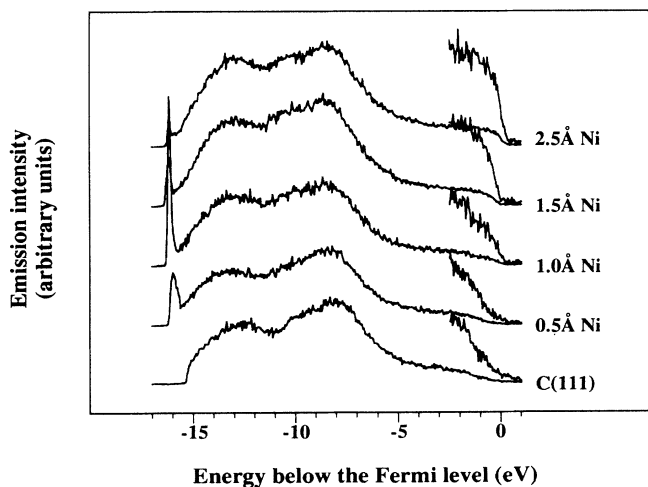


FIG. 6. Photoemission spectra of nickel on a hydrogen-free diamond (111) surface. A clear Fermi level can be discerned after deposition of  $1 \text{ \AA}$  of nickel. The diamond surface exhibits a negative electron affinity after deposition of the first  $0.5 \text{ \AA}$  nickel, as evidenced by a sharp peak at the low-energy end of the spectrum.

end of the spectrum appears, indicative of a negative-electron-affinity surface. This peak reaches a maximum for a film thickness of 1 Å. At that thickness a clear onset of emission due to the Fermi edge of the nickel film can be discerned. This suggests that continuous patches of nickel have formed, since a Fermi level is a macroscopic property of the metal. Upon nickel deposition a shift of  $\sim 0.4$  eV toward lower energies is observed in the spectrum of the underlying diamond, which indicates a change in the Fermi-level pinning of the diamond. A similar set of data is shown in Fig. 7 for nickel deposited on a surface that exhibited a negative electron affinity prior to deposition. The negative electron affinity appeared when LEED measurements were performed. Instead of increasing further, as might be expected based on the previous experiments, the negative-electron-affinity peak is now reduced after metal deposition. No shifts in the diamond spectra could be discerned upon nickel deposition. Schottky barrier heights were determined from the photoemission spectra, and are plotted as a function of film thickness in Fig. 8. This figure shows two distinctly different results. The upper data set was obtained from the surface that exhibited a negative electron affinity prior to nickel deposition, and a  $\sim 1.0$  eV Schottky barrier height is found for this surface. Nickel deposited on the argon-plasma-cleaned surface, however, resulted in a  $\sim 0.5$ -eV Schottky barrier height for the first monolayer of nickel. This Schottky barrier height was seen to increase to  $\sim 0.7$  eV upon further nickel deposition.

### B. Nickel on diamond (100)

Diamond (100) surfaces were cleaned *ex situ* and annealed in ultrahigh vacuum to temperatures ranging from 500°C to 1070°C. Auger, LEED, and photoemission spectroscopy were used to study the effect of the various anneals. Auger spectra, shown in Fig. 9, indicate that oxygen is present on the as-loaded surface. Only after an-

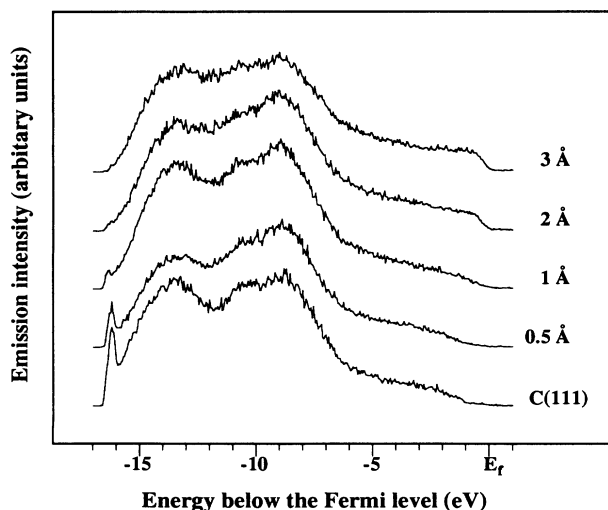


FIG. 7. Photoemission spectra of nickel deposited on a hydrogen-terminated diamond (111) surface. The negative electron affinity of the original surface is reduced upon nickel deposition.

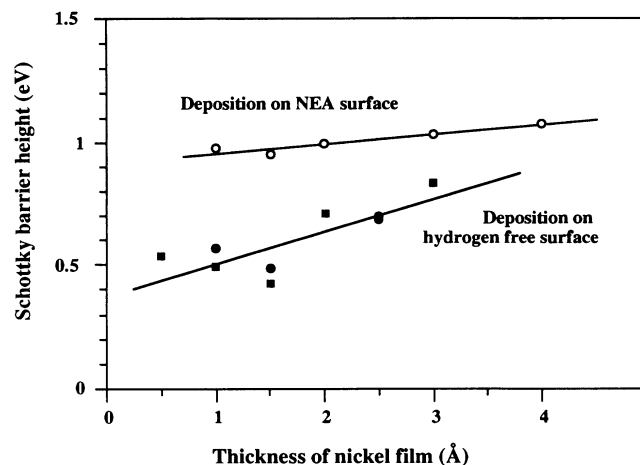


FIG. 8. Schottky barrier height of nickel on the diamond (111) surface as a function of metal thickness. The data in the upper curve (open circles) were obtained from a hydrogen-exposed surface while the data in the lower curve (black circles and squares) were obtained from hydrogen-free surfaces.

nealing to 900°C could a reduction in the oxygen signal be observed. This is in agreement with desorption studies performed by Thomas, Rudder and Markunas.<sup>53</sup> A faint  $2 \times 1$  reconstruction was observed, as determined by LEED. Further annealing to 1050°C resulted in a reduction of the amount of oxygen on the surface to below the detection limit of the Auger system, while the LEED pattern of the  $2 \times 1$  reconstruction was observed to sharpen. It should be mentioned that Auger spectroscopy measurements are not sensitive to hydrogen, and the presence of hydrogen is anticipated as described below.

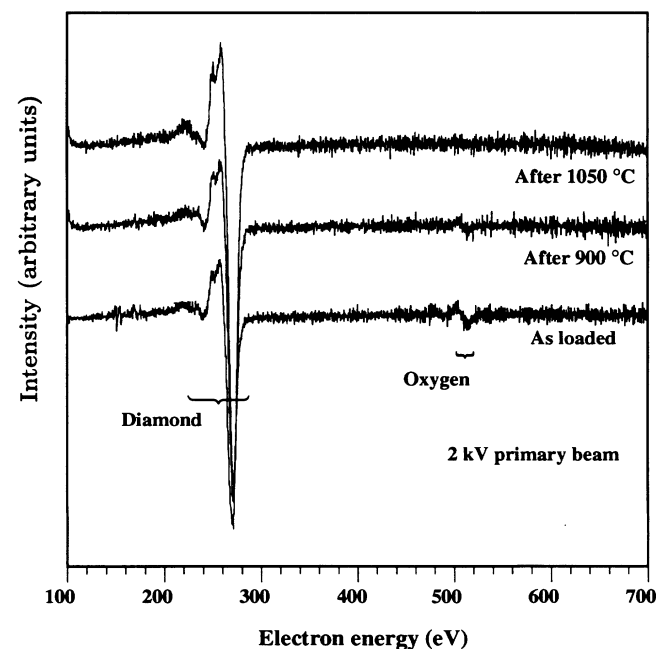


FIG. 9. Auger spectra obtained from the diamond (100) surface as a function of annealing temperature.

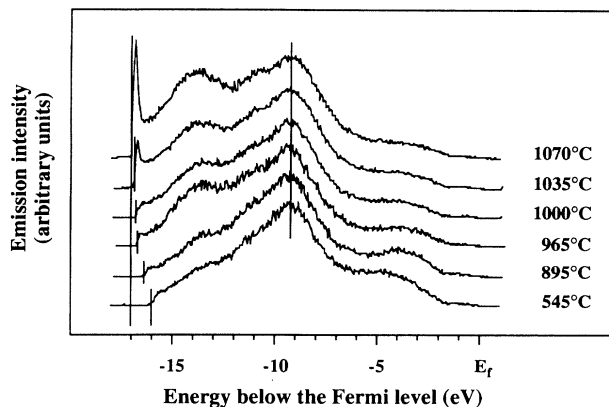


FIG. 10. Photoemission spectra obtained from the diamond (100) surface as a function of annealing temperature. The back edge is observed to shift with increasing annealing temperature. The shift is indicative of a lowering of the work function of the surface. The back edge has shifted by  $\sim 1$  eV for the high-temperature anneals. This resulted in a negative-electron-affinity surface, as evidenced by the sharp peak. The spectra have been lined up according to the feature indicated by the solid line.

Photoemission spectra of the diamond (100) surface as a function of annealing temperature were obtained in a parallel study and are shown in Fig. 10. These spectra exhibited small but inconsistent shifts in energy on the order of 0.2 eV and are therefore aligned with respect to the feature at 8.3 eV below the valence-band edge. As can be seen in the figure, the back edge of the spectra shifts by  $\sim 1$  eV toward lower energies as the diamond (100) is annealed to higher temperatures. This signifies a lowering of the work function and consequently a lowering of the electron affinity. After the 1035°C anneal a peak appears in the spectra at low electron energies, indicative of a negative-electron-affinity surface. The peak increased in height upon further annealing to 1070°C.

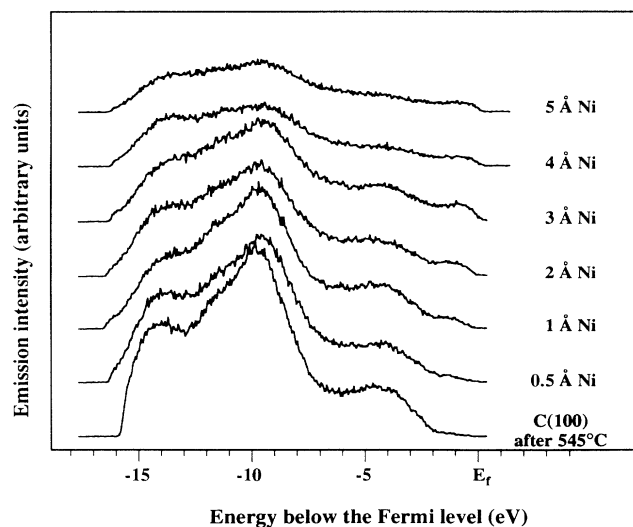


FIG. 11. Photoemission spectra of nickel deposited on a diamond (100) substrate after annealing at 545°C.

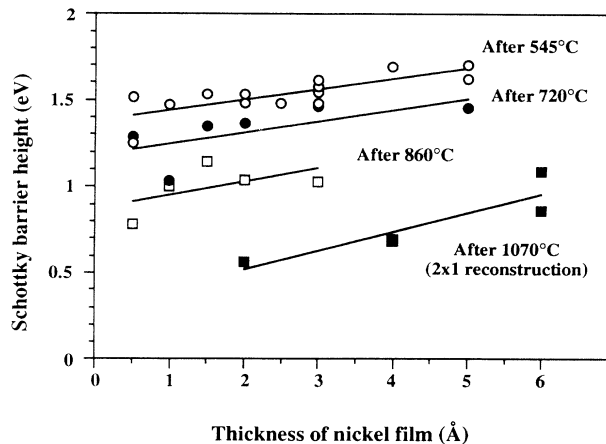


FIG. 12. Schottky barrier height of nickel on diamond (100) as a function of metal thickness. The different data sets were obtained after the substrates had been annealed to the temperatures indicated in the figure.

Nickel was deposited on surfaces that had been annealed to temperatures ranging from 545°C to 860°C and photoemission spectra were obtained after each deposition. A typical series of spectra is shown in Fig. 11. Although the back edge of the spectra is observed to shift toward lower energies, the negative-electron-affinity effect does not appear upon nickel deposition. The Schottky barrier heights determined from these spectra are plotted as a function of metal thickness in Fig. 12. In addition, nickel was deposited on a  $2 \times 1$  reconstructed surface, obtained by annealing the surface to 1070°C. After each deposition of nickel on this surface, the film was annealed to  $\sim 370^\circ\text{C}$  to obtain epitaxial growth. As can be seen in Fig. 13, the negative-electron-affinity peak was slightly reduced, but remained visible after 2 Å of nickel had been deposited. After further nickel deposition the peak disappeared. After  $\sim 35$  Å of nickel had been deposited, the sample exhibited a (100)  $1 \times 1$  LEED pattern, indicating that the film had grown epitaxially. Schottky barrier

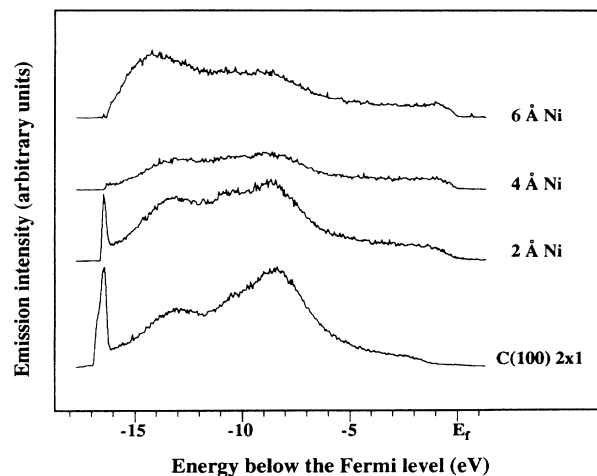


FIG. 13. Photoemission spectra of nickel deposited on a  $2 \times 1$  reconstructed diamond (100) surface.

heights obtained from these photoemission spectra are also plotted in Fig. 12. As can be seen in the figure, the Schottky barrier height is reduced from  $\sim 1.5$  for nickel on the  $545^\circ\text{C}$  annealed surface to  $\sim 1.0$  eV for nickel on the  $860^\circ\text{C}$  annealed surface, while an even lower Schottky barrier height of  $\sim 0.7$  eV was found for nickel grown epitaxially on the  $2\times 1$  reconstructed surface.

#### IV. DISCUSSION

##### A. Nickel on diamond (111)

From the results presented here, the Schottky barrier height for nickel on the hydrogen-free diamond (111) surface was found to be  $\sim 0.5$  eV. Theoretical calculations performed by Erwin and Pickett indicate, however, that the interface structure with the lowest formation energy, nickel in the "tetrahedral" position, results in a Schottky barrier height of  $< 0.1$  eV. It should be noted, however, that the formation energy of the tetrahedral structure (0.97 eV/atom) is almost identical to the formation energy of the "in-hollow" structure (1.06 eV/atom). There is, however, a significant difference between the calculated Schottky barrier heights for these two structures. For the tetrahedral position, which is energetically the most favorable, a Schottky barrier height of  $< 0.1$  eV is found, while the in-hollow position leads to a predicted Schottky barrier height of 0.8 eV. Since nickel is not expected to grow epitaxially at room temperature on the (111) surface,<sup>31</sup> and in light of the fact that the two proposed formations are so close in formation energy, we suggest that both formations occur at the interface. That would result in an effective Schottky barrier height between  $< 0.1$  and 0.8 eV, which is in general agreement with our experimental value of 0.5 eV.

The influence of interfacial hydrogen on the Schottky barrier has been studied by Lambrecht,<sup>37</sup> who performed calculations on the copper-diamond (111) interface. Copper, like nickel, has a fcc lattice that closely matches the lattice of diamond, and the two elements are expected to behave in a very similar fashion. This is borne out by the fact that the calculations of Lambrecht for copper on diamond (111) lead to very similar results as the ones done on nickel by Erwin and Pickett. Lambrecht finds a nearly zero Schottky barrier height for copper in the tetrahedral position, while a Schottky barrier height of  $\sim 0.5$  eV is found for the in-hollow position. His calculations of copper on hydrogen-terminated (111) diamond, however, indicate a theoretical Schottky barrier of more than 1 eV. This agrees with our results, which suggest that the presence of hydrogen at the surface leads to a higher Schottky barrier.

The possibility was considered that the negative electron affinity observed after the nickel deposition was the result of a lowering of the work function of the surface due to the nickel. A similar effect has been reported for titanium on the diamond (111) surface.<sup>56</sup> In order for this to occur, the sum of the Schottky barrier height and the metal work function has to be less than the band gap of the semiconductor, as illustrated in Fig. 14. With a Schottky barrier height of 0.5 eV and a band gap of 5.47

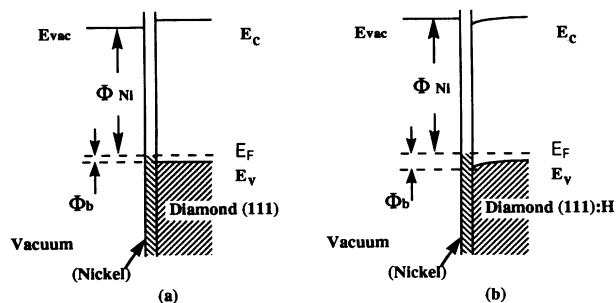


FIG. 14. Band diagrams of the nickel-diamond interface. In (a) the sum of the Schottky barrier height and work function for nickel on diamond is less than the band gap of diamond, resulting in a negative electron affinity, while in (b) the sum is larger than the band gap, which results in a positive electron affinity.

eV, that would mean that the nickel work function would have to be less than 5.0 eV. The reported value for the work function of polycrystalline nickel films is  $5.15 \pm 0.1$  eV.<sup>57</sup> It is of interest to note, however, that the presence of carbon contamination tends to lower the work function of the nickel.<sup>58</sup> This suggests the possibility that the carbon of the diamond affects the work function of the first layer of nickel.

For the nickel deposited on the hydrogen-terminated (111) surface an increased Schottky barrier height of  $\sim 1.0$  eV is observed. According to our model this would lead to an increased electron affinity, from a negative affinity to a 0.5-eV positive affinity. This is in agreement with the observed disappearance of the negative-electron-affinity feature upon nickel deposition, as can be seen in Fig. 7. The difference in electron affinity for nickel deposited on the clean (111) surface and nickel on the hydrogen-terminated (111) surface is therefore attributed to the difference in Schottky barrier heights.

##### B. Nickel on diamond (100)

As discussed in the Introduction, the unreconstructed diamond (100) can be obtained by terminating the surface with either a dihydride or an oxide. It is unlikely that the oxygen observed in the Auger spectra is due to adsorbed species such as  $\text{CO}_2$  or  $\text{H}_2\text{O}$  since oxygen remains present on the (100) surface after a  $900^\circ\text{C}$  anneal. In addition, the removal of oxygen is observed to coincide with the appearance of the  $2\times 1$  reconstruction, which suggest that this oxygen is chemically bonded to the surface in one of the two structures proposed by Thomas, Rudder, and Markunas<sup>53</sup> [see Figs. 2(b) and 2(c)]. The presence of a dihydride phase illustrated in Fig. 2(a) cannot be ruled out, however, since Auger spectroscopy is not sensitive to hydrogen, and it is likely that both hydrogen and oxygen occur at the surface. We attribute the lowering of the work function of the diamond (100) surface as a function of annealing temperature to the desorption of the adsorbed species. The negative electron affinity, observed on the  $2\times 1$  reconstructed surface, is attributed to a monohydride-terminated surface structure. This conclusion is based on preliminary pseudo-potential calcula-

tions performed by Zhang, Wensell, and Bernholc which indicate that the  $2 \times 1$  monohydride-terminated surface exhibits a 0.62-eV negative electron affinity, whereas a positive electron affinity was found for the hydrogen-free surface.<sup>59</sup> We assign, therefore, a Schottky barrier height of  $\sim 1.5$  eV to nickel on an oxygen- and/or hydrogen-terminated diamond (100) surface with the possibility that a dihydride phase is present on the surface as well. Increasing the annealing temperature of the surface to 860°C prior to deposition resulted in a lower Schottky barrier height of  $\sim 1$  eV. An even lower Schottky barrier height of  $\sim 0.7$  eV was found for nickel grown epitaxially on a  $2 \times 1$  reconstructed, monohydride-terminated (100) surface. Although in the latter case the nickel film was annealed after growth, we interpret the lower Schottky barrier height as a continuation of the trend that was observed in the other samples. The Schottky barrier height on both the reconstructed and the unreconstructed surfaces is too large to allow a metal-induced negative electron affinity. The measured Schottky barriers for the nickel-diamond (100) interfaces do not agree with theoretical calculations performed by Erwin and Pickett, which predict a zero Schottky barrier height.<sup>32–35</sup> This can be attributed to the fact that their calculations are based on an ideal, hydrogen-free diamond (100) surface whereas in our experiments oxygen and hydrogen were present at the interface. To our knowledge there are no theoretical studies on the effects of interfacial hydrogen or oxygen on the Schottky barrier height of metals on the diamond (100) surface.

## V. CONCLUSIONS

Using photoemission spectroscopy we have investigated the nickel-diamond interface. A Schottky barrier height of 0.5–0.7 eV was found for nickel on a

hydrogen-free diamond (111) surface. When hydrogen was present on the surface an increased Schottky barrier height of  $\sim 1.0$  eV was found. This agrees with theoretical calculations performed on the copper-diamond (111) interface. Nickel deposited on the hydrogen-free surface resulted in a negative-electron-affinity surface, which is attributed to the low Schottky barrier for that interface. Diamond (100) surfaces were subjected to various anneals, which resulted in a reduction of oxygen bonded to the surface and a lowering of the electron affinity. Annealing the diamond (100) surface to  $\sim 1000^\circ\text{C}$  resulted in a monohydride-terminated,  $2 \times 1$  reconstructed surface which exhibited a negative electron affinity. Schottky barrier heights for nickel on the diamond (100) surface were observed to vary from  $\sim 1.5$  eV for the 545°C annealed surface, to  $\sim 0.7$  eV for the  $2 \times 1$  reconstructed surface. From these results we conclude that the presence of interfacial hydrogen and/or oxygen results in an increased Schottky barrier height for nickel on both the (111) and the (100) surface. These results suggest that surface preparation can significantly affect the Schottky barrier height for metals on diamond. We therefore attribute the large variation in reported Schottky barrier heights, as discussed in the Introduction, to differences in surface preparations.

## ACKNOWLEDGMENTS

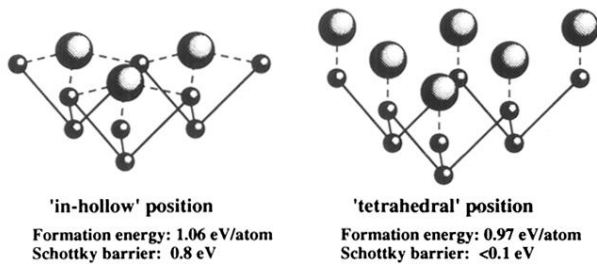
We acknowledge helpful discussions with T. P. Humphreys and R. E. Thomas of the Research Triangle Institute, technical assistance of D. B. Aldrich and T. P. Schneider, and K. Das of Kobe Research for guidance on substrate preparations. This work was supported in part by the Office of Naval Research through Grants N0014-92-J-1477 and N0014-92-J-1604, and the National Science Foundation through Grant No. DMR-9204285.

<sup>1</sup>H. Shiomi, Y. Nishibayashi, and N. Fujimori, *Jpn. J. Appl. Phys.* **28**, L2153 (1989).  
<sup>2</sup>H. Shiomi, Y. Nishibayashi, and N. Fujimori, *Jpn. J. Appl. Phys.* **29**, L2163 (1990).  
<sup>3</sup>G. S. Gildenblat, S. A. Grot, C. W. Hatfield, and A. R. Badzian, *IEEE Electron Device Lett.* **12**, 37 (1991).  
<sup>4</sup>W. Tsai, M. Delfino, D. Hodul, M. Riazat, L. Y. Ching, G. Reynolds, and C. B. Cooper III, *IEEE Electron Device Lett.* **12**, 157 (1991).  
<sup>5</sup>H. Kiyota, K. Okano, T. Iwasaki, H. Izumiya, Y. Akiba, T. Kurosu, and M. Iida, *Jpn. J. Appl. Phys.* **30**, 2015 (1991).  
<sup>6</sup>J. F. Prins, *Appl. Phys. Lett.* **41**, 950 (1982).  
<sup>7</sup>Y. Tzeng, T. H. Lin, J. L. Davidson, and L. S. Tan, *1987 University/Government/Industry Microelectronics Symposium*, edited by L. Fuller (IEEE, New York, 1987), p. 290.  
<sup>8</sup>K. Das, V. Venkatesan, K. Miyata, D. L. Dreifus, and J. T. Glass, *Thin Solid Films* **212**, 19 (1992).  
<sup>9</sup>F. Fang, C. A. Hewett, M. G. Fernandes, and S. S. Lau, *IEEE Trans. Electron Devices* **36**, 1783 (1989).  
<sup>10</sup>M. W. Geis, D. D. Rathman, D. J. Ehrlich, R. A. Murphy, and W. T. Lindley, *IEEE Electron Device Lett.* **8**, 341 (1987).

<sup>11</sup>G. S. Gildenblat, S. A. Grot, C. R. Wronski, A. R. Badzian, T. Badzian, and R. Messier, *Appl. Phys. Lett.* **53**, 586 (1988).  
<sup>12</sup>G. S. Gildenblat, S. A. Grot, C. W. Hatfield, A. R. Badzian, and T. Badzian, *IEEE Electron Device Lett.* **11**, 371 (1990).  
<sup>13</sup>J. W. Glesener, A. A. Morrish, and K. A. Snail, *J. Appl. Phys.* **70**, 5144 (1991).  
<sup>14</sup>G. H. Glover, *Solid-State Electron.* **16**, 973 (1973).  
<sup>15</sup>S. A. Grot, G. S. Gildenblat, C. W. Hatfield, C. R. Wronski, A. R. Badzian, T. Badzian, and R. Messier, *IEEE Electron Device Lett.* **11**, 100 (1990).  
<sup>16</sup>M. C. Hicks, C. R. Wronski, S. A. Grot, G. S. Gildenblat, A. R. Badzian, T. Badzian, and R. Messier, *J. Appl. Phys.* **65**, 2139 (1989).  
<sup>17</sup>P. R. de la Houssaye, C. Pechina, C. A. Hewett, R. G. Wilson, and J. R. Zeidler, in *New Diamond Science and Technology*, edited by R. Messier, J. T. Glass, J. E. Butler, and R. Roy (Materials Research Society, Pittsburgh, 1991), p. 1113.  
<sup>18</sup>T. P. Humphreys, J. V. LaBrasca, R. J. Nemanich, K. Das, and J. B. Posthill, *Jpn. J. Appl. Phys. A* **30**, L1409 (1991).  
<sup>19</sup>M. Marchywka, J. F. Hochedez, M. W. Geis, D. G. Socker, D. Moses, and R. T. Goldberg, *Appl. Opt.* **30**, 5011 (1991).

- <sup>20</sup>K. L. Moazed, R. Nguyen, and J. R. Zeidler, *IEEE Electron Device Lett.* **9**, 350 (1988).
- <sup>21</sup>K. L. Moazed, J. R. Zeidler, and M. J. Taylor, *J. Appl. Phys.* **68**, 2246 (1990).
- <sup>22</sup>K. L. Moazed, J. R. Zeidler, and M. J. Taylor in *Diamond, Silicon Carbide and Related Wide Bandgap Semiconductors*, edited by J. T. Glass, R. F. Messier, and N. Fujimori, MRS Symposia Proceedings No. 162 (Materials Research Society, Pittsburgh, 1990), p. 347.
- <sup>23</sup>Y. Mori, H. Kawarada, and A. Hiraki, *Appl. Phys. Lett.* **58**, 940 (1991).
- <sup>24</sup>J. F. Prins, *J. Phys. D* **22**, 1562 (1989).
- <sup>25</sup>H. Shiomi, H. Nakahata, T. Imai, Y. Nishibayashi, and N. Fujimori, *Jpn. J. Appl. Phys.* **28**, 758 (1989).
- <sup>26</sup>T. Tachibana, B. E. Williams, and J. T. Glass, *Phys. Rev. B* **45**, 11 968 (1992).
- <sup>27</sup>T. Tachibana, B. E. Williams, and J. T. Glass, *Phys. Rev. B* **45**, 11 975 (1992).
- <sup>28</sup>G. Zhao, T. Stacy, E. J. Charlson, E. M. Charlson, C. H. Chao, M. Hajsaid, and J. Meese, *Appl. Phys. Lett.* **61**, 1119 (1992).
- <sup>29</sup>S. A. Grot, S. Lee, G. S. Gildenblat, C. W. Hatfield, C. R. Wronski, A. R. Badzian, T. Badzian, and R. Messier, *J. Mater. Res.* **5**, 2497 (1990).
- <sup>30</sup>P. G. Lurie and J. M. Wilson, *Surf. Sci.* **65**, 453 (1977).
- <sup>31</sup>P. Pavlidis, *Thin Solid Films* **42**, 221 (1977).
- <sup>32</sup>S. C. Erwin and W. E. Pickett, *Surf. Coat. Technol.* **47**, 487 (1991).
- <sup>33</sup>S. C. Erwin and W. E. Pickett, *Solid State Commun.* **81**, 891 (1992).
- <sup>34</sup>W. E. Pickett and S. C. Erwin, *Phys. Rev. B* **41**, 9756 (1990).
- <sup>35</sup>W. E. Pickett and S. C. Erwin, *Superlatt. Microstruct.* **7**, 335 (1990).
- <sup>36</sup>W. E. Pickett, M. R. Pederson, and S. C. Erwin, *Mater. Sci. Eng. B* **14**, 87 (1992).
- <sup>37</sup>W. R. L. Lambrecht, *Physica B* **185**, 512 (1993).
- <sup>38</sup>A. V. Hamza, G. D. Kubiak, and R. H. Stulen, *Surf. Sci.* **206**, 1 (1988).
- <sup>39</sup>B. B. Pate, M. H. Hecht, C. Binns, I. Lindau, and W. E. Spicer, *J. Vac. Sci. Technol.* **21**, 364 (1982).
- <sup>40</sup>B. B. Pate, *Surf. Sci.* **165**, 83 (1986).
- <sup>41</sup>B. B. Pate, B. J. Waclawski, P. M. Stefan, C. Binns, T. Ohta, M. H. Hecht, P. J. Jupiter, M. L. Shek, D. T. Pierce, N. Swanson, R. J. Celotta, G. Rossi, I. Lindau, and W. E. Spicer, *Physica B* **117&118** 783 (1983).
- <sup>42</sup>F. J. Himpsel, J. A. Knapp, J. A. van Vechten, and D. E. Eastman, *Phys. Rev. B* **20**, 624 (1979).
- <sup>43</sup>F. J. Himpsel, D. E. Eastman, and J. F. van der Veen, *J. Vac. Sci. Technol.* **17**, 1085 (1980).
- <sup>44</sup>F. J. Himpsel, J. F. van der Veen, and D. E. Eastman, *Phys. Rev. B* **22**, 1967 (1980).
- <sup>45</sup>F. J. Himpsel, P. Heimann, and D. E. Eastman, *Solid State Commun.* **36**, 631 (1980).
- <sup>46</sup>B. B. Pate, W. E. Spicer, T. Ohta, and I. Lindau, *J. Vac. Sci. Technol.* **17**, 1087 (1980).
- <sup>47</sup>B. B. Pate, P. M. Stefan, C. Binne, P. J. Jupiter, M. L. Shek, I. Lindau, and W. E. Spicer, *J. Vac. Sci. Technol.* **19**, 349 (1981).
- <sup>48</sup>J. van der Weide and R. J. Nemanich, *Appl. Phys. Lett.* **62**, 1878 (1993).
- <sup>49</sup>A. V. Hamza, G. D. Kubiak, and R. H. Stulen, *Surf. Sci.* **237**, 35 (1990).
- <sup>50</sup>Y. L. Yang and M. P. D'Evelyn, *J. Am. Chem. Soc.* **114**, 2796 (1992).
- <sup>51</sup>P. C. Yang, W. Zhu, and J. T. Glass, *J. Mater. Res.* **9** (to be published).
- <sup>52</sup>Y. L. Yang, L. M. Struck, L. F. Sutcu, and M. P. D'Evelyn, *Thin Solid Films* **225**, 203 (1993).
- <sup>53</sup>R. E. Thomas, R. A. Rudder, and R. J. Markunas, *J. Vac. Sci. Technol. A* **10**, 2451 (1992).
- <sup>54</sup>C. A. Mead and T. C. McGill, *Phys. Lett.* **58A**, 249 (1976).
- <sup>55</sup>J. van der Weide and R. J. Nemanich, in *Applications of Diamond Films and Related Materials*, edited by Y. Tzeng, M. Yoshikawa, M. Murakawa, and A. Feldman (Elsevier, Amsterdam, 1991), p. 359.
- <sup>56</sup>J. van der Weide and R. J. Nemanich, *J. Vac. Sci. Technol. B* **10**, 1940 (1992).
- <sup>57</sup>D. E. Eastman, *Phys. Rev. B* **2**, 1 (1970).
- <sup>58</sup>C. Weiser, *Surf. Sci.* **20**, 143 (1970).
- <sup>59</sup>Z. Zhang, M. G. Wensell, and J. Bernholc (private communication).

Nickel on (111) diamond



Nickel on (100) diamond

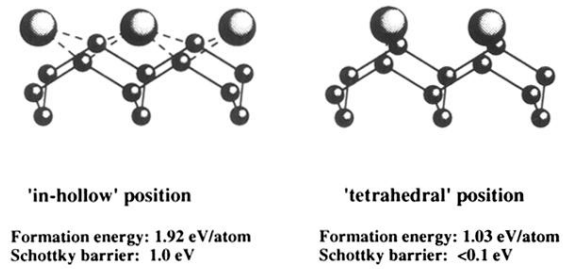
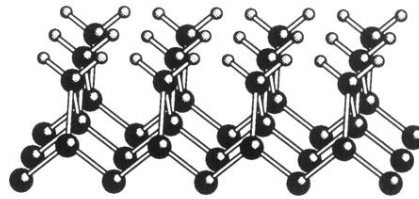
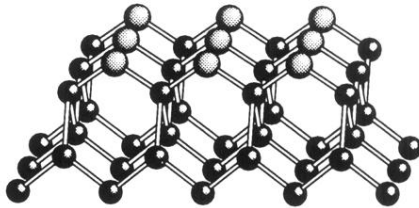


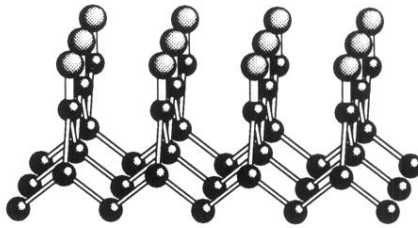
FIG. 1. Various configurations of nickel on diamond (111) and (100) as studied in Refs. 32–34, and 36.



(a) Diamond (100) 1x1:2H Dihydride structure



(b) Diamond (100) 1x1:O Bridging structure



(c) Diamond (100) 1x1:O Double-bonded structure

FIG. 2. (a) Dihydride- and (b) and (c) oxygen-terminated diamond (100) surfaces with a  $1 \times 1$  surface structure.